

Anatomical Predictions of Hearing in the North Atlantic Right Whale

SUSAN E. PARKS,* DARLENE R. KETTEN, JENNIFER T. O'MALLEY,
AND JULIE ARRUDA

Woods Hole Oceanographic Institution, Woods Hole, Massachusetts

ABSTRACT

Some knowledge of the hearing abilities of right whales is important for understanding their acoustic communication system and possible impacts of anthropogenic noise. Traditional behavioral or physiological techniques to test hearing are not feasible with right whales. Previous research on the hearing of marine mammals has shown that functional models are reliable estimators of hearing sensitivity in marine species. Fundamental to these models is a comprehensive analysis of inner ear anatomy. Morphometric analyses of 18 inner ears from 13 stranded North Atlantic right whales (*Eubalaena glacialis*) were used for development of a preliminary model of the frequency range of hearing. Computerized tomography was used to create two-dimensional (2D) and 3D images of the cochlea. Four ears were decalcified and sectioned for histologic measurements of the basilar membrane. Basilar membrane length averaged 55.7 mm (range, 50.5 mm–61.7 mm). The ganglion cell density/mm averaged 1,842 ganglion cells/mm. The thickness/width measurements of the basilar membrane from slides resulted in an estimated hearing range of 10 Hz–22 kHz based on established marine mammal models. Additional measurements from more specimens will be necessary to develop a more robust model of the right whale hearing range. *Anat Rec*, 290:734–744, 2007. © 2007 Wiley-Liss, Inc.

Key words: cetacean; hearing; cochlea; basilar membrane; baleen whale

North Atlantic right whales (*Eubalaena glacialis*) are among the most endangered mysticetes (baleen whales) in the world. Although these whales have been protected from whaling for much of this century, today fewer than 350 remain (Hamilton and Martin, 1999; Knowlton and Kraus, 2001). Over 30% of known right whale mortalities in the past 30 years have been attributed to collisions with vessels or entanglement in fishing gear (Kraus, 1990; Kenney and Kraus, 1993; Laist et al., 2001). Reducing human contributions to mortality is imperative for survival of this species. At present, we do not know whether the whales are able to hear or localize an approaching vessel. Failure to hear vessels could be due to limitations of hearing in right whales or acoustic propagation anomalies (e.g., the Llyod mirror effect; Richardson et al., 1995) near the surface. One method proposed to reduce vessel strikes is to equip ships with alarm devices that alert whales to an approaching vessel (Nowacek et al., 2003). Similarly, development of right whale targeted acoustic pinger systems for fishing gear could reduce mortality from entanglement. Thus, infor-

mation about the frequency range and sensitivity of hearing in right whales is necessary to determine whether hearing limitations play a role in vessel collisions, to identify appropriate frequency bands for acoustic pinger stimulus development, and to determine what anthropogenic noise sources may be affecting hearing and acoustic communication in this species. This study

Grant sponsor: The Northeast Consortium; Grant numbers: 02-560 and 03-675; Grant sponsor: Penzance Foundation through the Right Whale Initiative of the WHOI Ocean Life Institute.

*Correspondence to: Susan E. Parks, Pennsylvania State University, Applied Research Laboratory, P.O. Box 30 State College, PA 16804-0030. E-mail: sep20@psu.edu

Received 2 March 2007; Accepted 6 March 2007

DOI 10.1002/ar.20527

Published online in Wiley InterScience (www.interscience.wiley.com).

uses anatomical measurements to predict the hearing abilities of right whales.

HEARING STUDIES IN CETACEANS

Most hearing data from cetaceans come from studies with small captive toothed-whales. Audiograms have been made from 10 of these species (Au, 2000). Right whales are not amenable to conventional behavioral or electrophysical methods for measuring hearing because of their large size and endangered status. The frequency range of best hearing is commonly thought to overlap with that of stereotypical species calls (Sales and Pye, 1974). Most baleen whale vocalizations have the majority of their energy below 1 kHz. The average ambient noise levels in all 1/3-octave bands below 1 kHz are higher than 75 dB re 1 μ Pa (Urick, 1983). Ambient noise levels may limit the real world detection threshold for baleen whales. In the field, information on baleen hearing abilities in the context of ambient noise can be obtained from behavioral responses of whales to playback stimuli. Playback experiments with several species have indicated good directional hearing capabilities in baleen whales based on orientation toward and localization of conspecific calls (Clark and Clark, 1980; Watkins, 1981; Tyack, 1983; Parks, 2003) and clear responses of gray whales (*Eschrichtius robustus*) to the calls of killer whale predators (*Orcinus orca*) (Cummings and Thompson, 1971). Studies of baleen whale response to anthropogenic noise sources documented response at frequencies up to at least 15 kHz (Watkins, 1986). One playback experiment estimated the broadband received level of sound necessary to elicit an approach response from humpback whales (*Megaptera novaeangliae*) to be 102 dB re 1 μ Pa for feeding sounds (Frankel et al., 1995).

ANATOMICAL MODELING FOR MARINE MAMMAL HEARING

Comparative anatomical studies have identified structural correlates to frequency range and hearing sensitivity in multiple mammalian species (Echteler et al., 1994). Functional studies of the inner ear focus on resonance characteristics of the basilar membrane. Models have been developed to predict the frequency range of hearing for cetaceans in particular based on basilar membrane measurements (Ketten and Wartzok, 1990). Position–frequency maps and basilar membrane elasticity measurements from humans as well as other mammal and bird species were used by Greenwood to derive formulae for predicting frequency maxima, minima, and distribution along the length of the basilar membrane for land mammals (Greenwood, 1961, 1962, 1990). Other estimates of overall hearing ranges have been based on either cochlear length or length and width (Manley, 1971; West, 1985). Fay's (1992) extrapolation of Greenwood's work shows that estimators derived from even a single basilar membrane dimension provide very close approximations of psychophysical measures of hearing for most land mammals, referred to as generalists. However, these formulae provide a poor fit to hearing curves of species with specialized hearing, e.g., the horseshoe bat (*Rhinolophus ferrumequinum*) and the mole rat (*Spalax ehrenbergi*), largely because these species have a basilar membrane stiffness gradient that differs from

the generalist basilar membrane (Echteler et al., 1994). Species with high frequency hearing tend to have comparatively narrow and thick basilar membranes with better developed outer spiral laminae that continue through most of the cochlear duct (Ketten, 1984). In species with ears specialized for low frequency hearing, the basilar membrane is generally wider and thinner, with the outer spiral laminae thinner and if present, located only in the basal region of the cochlea (Echteler et al., 1994). Measurements of basal and apical stiffness of the basilar membrane, which can be approximated by the ratio of thickness to width, appear to predict the upper and lower frequency limits equally well for both generalists and specialist ears (Ketten and Wartzok, 1990), and comparative anatomical studies of cetacean and terrestrial mammalian ears demonstrate significant structural variants unique to cetacean ears (Ketten, 1992).

Whale ears have the same basic components as land mammal ears but they also have adaptations to the aquatic environment that require more comprehensive modeling. Generalized morphometric models for land mammals provide a procedural or mechanistic basis for marine mammal analyses, but these must be modified to accommodate structural differences in whale ears compared with those from typical land mammals. Whale basilar membrane thickness and width differ from that typical of land mammal ears, and consequently, their basilar membranes do not follow the generalist stiffness gradients for their membrane lengths. Therefore, estimates using generic land mammal formulae based on length alone are incorrect for cetaceans (Ketten, 1984).

The appropriateness of a more comprehensive model for whales was first demonstrated in a structural analysis of the cochlea of 12 odontocete species (Ketten, 1984; Ketten and Wartzok, 1990). The results of these studies showed that a combination of four measurements of cochlear structure (basilar membrane dimensions, laminar extent, membrane pitch, and basal turn ratio) allowed for excellent prediction of the primary bands of ultrasonic hearing in odontocetes (Ketten, 1984; Ketten and Wartzok, 1990).

This study describes the anatomy of right whale ears and uses the model (Ketten, 1994) based on the measurements of the basilar membrane pitch, basal turn ratio, and basilar membrane dimensions to estimate their frequency range of hearing. The anatomy of the right whale ear indicates that they are specialized for low frequency hearing.

MATERIALS AND METHODS

Specimen Collection and Preservation

The endangered status of the North Atlantic right whale has led to systematic necropsies on all recovered dead right whales (Moore et al., 2004). Right whale temporal bones have been routinely collected from necropsies since 1989. Ears were either frozen shortly after collection or placed in a buffered 10% formalin solution. Preservation condition ranged from code 2 to code 4 (2, fresh; 3, decomposed; 4, severely decomposed) (Moore et al., 2004). A total of 18 ears were analyzed from 13 different individuals (Table 1). All ears were computer tomography (CT) scanned, and four ears were further processed into slides for histology.

TABLE 1. Specimens measured for this study^a

Specimen	Stranding	Age	Sex	Length (cm)	Code	Preservation	CT	Histology
Eg1	1/3/1989	Calf	M	425	2	Formalin	X	X
EG 4/5*	2/22/1996	Calf	M	407	3	Formalin	X	X
EG 6*	1/2/1996	Calf	F	478	3	Formalin	X	
EG 7*	7/17/1995	2 1/2	M	1030	3	Formalin	X	
EG 8	1/30/1996	Adult	M	1415	3	Formalin	X	
EG 9	2/19/1996	Calf	F	513	3	Formalin	X	X
EG 10	10/29/1999	10	F	1350	4	Frozen	X	
EG 11	3/9/1996	4+	M	1270	3	Frozen	X	
EG 13/14	1/9/1997	Calf	M	417	3	Formalin	X	
EG 16*	8/19/1997	Adult	F	1259	2	Frozen	X	
EG 18*	4/20/1999	Adult	F	1370	2	Formalin	X	X
EG 19	3/18/2001	Calf	M	660	3	Formalin	X	
EG 20	6/18/2001	Calf	F	1050	3	Frozen	X	

^aData given indicate the date of the stranding, the age (calf < 6 months in age, adult > 8 years of age) of the whale at time of death, sex, total body length measured from snout to fluke notch, state of preservation of the specimen at time of necropsy (Code: 1 = best, 4 = worst), and whether the specimen was analyzed using CT and histology. Asterisks indicate that both ears were analyzed from these specimens.

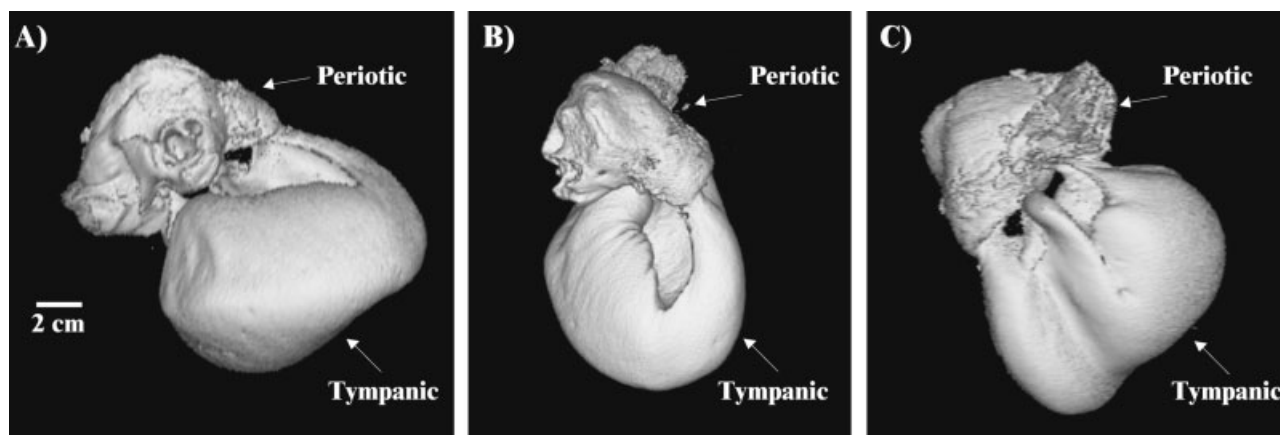


Fig. 1. A three-dimensional (3D) reconstruction of the entire left temporal bone complex from specimen EG 5. The reconstruction is from 0.5-mm sections of computed tomography scans. The tympanic and periotic are labeled in each image. **A:** Medial view. **B:** Anterior view. **C:** Lateral view.

CT Measurements

Each specimen was imaged using CT scanning. The specimens were scanned with a Siemens Spiral Plus 4 CT (Massachusetts Eye and Ear Infirmary) or a Siemens Emotion Spiral CT and Volume Zoom scanner (Woods Hole Oceanographic Institution). Scans were obtained with a 1-mm spiral ultra-high-resolution protocol and reconstructed at 0.5-mm slice thickness. Three specimens were additionally scanned using a 0.5-mm spiral acquisition. Both 2D and 3D representations of the scan data were used for measuring the cochlear anatomy of the right whale ears (Figs. 1–4).

The number of turns in each cochlea was determined from 3D reconstructions of the cochlear duct oriented for a top-down, apex to base, view of the cochlea (Fig. 3B). Cochlear lengths were determined by measuring the length of cochlear turn radii for multiple positions in the cochlea from 2D paramodiolar (Fig. 4) cross-sections. The paramodiolar slices were formatted to be perpendicular to the longer axis of the basal turn. These values were then used to calculate the axial pitch, basal ratio,

and the length of the cochleae. The length calculations were made using the following formulae (Ketten et al., 1998):

$$(1) \text{ For } r = a\theta$$

$$(2)$$

$$z = \sqrt{\left\{ \frac{a}{2} \left[\left(\theta \sqrt{\theta^2 + 1} \right) + \text{Ln} \left(\theta + \sqrt{\theta^2 + 1} \right) \right] \right\}^2 + h^2}$$

where z = cochlear length, r = radius at angular displacement θ in radians, a = constant that determines the size of the spiral, and h = axial height of the spiral (Fig. 5).

The 3D reconstructions of each cochlea were measured directly to compare the observed cochlear length from the CT scan with calculated cochlear length based on 2D radii measurements. The basal diameter of the cochlea was measured from the 3D reconstructions in the same orientation as the radial cross-sections. Small differences among these measures are to be expected because the

3D images are oriented as flat projections and include the basal hook of the cochlear spiral, while the calculated lengths include the cochlear rise but do not include the basal hook length.

Gross Dissection and Histology Measurements

Specimens with evidence of preservation of the vestibulocochlear (VIIIth cranial) nerve and of the basilar

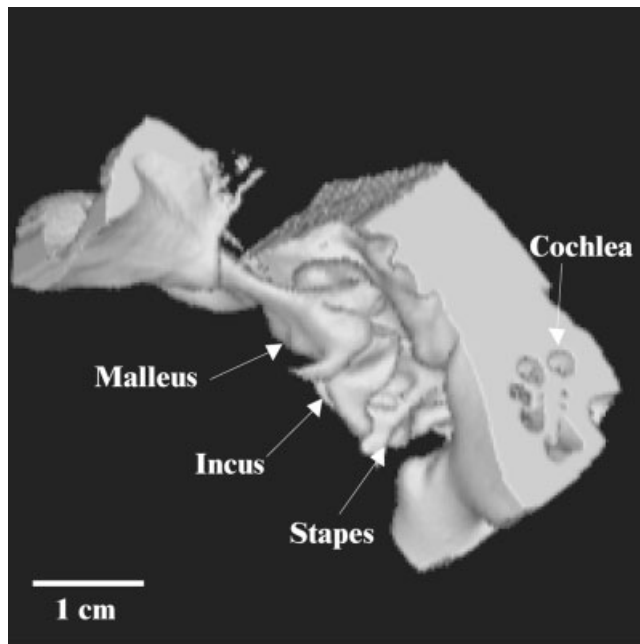


Fig. 2. A three-dimensional (3D) reconstruction of the ossicular chain from a right whale. The figure shows the in situ orientation, the angle between ossicles, as well as the position of the ossicles relative to the cochlea. A cross-section through the cochlea can be seen on the right side of the figure. This cross-section is approximately the same orientation as the cross-section shown in Figure 4.

membrane based on the CT scan images were selected for further processing. These specimens were dissected, which involved defrosting frozen specimens in 10% buffered formalin solution and removal of all remaining external soft tissue (Fig. 6). The remaining tissues were measured and weighed. The periotic and tympanic bones were then separated and the bony flanges were removed from the periotic by use of a handsaw to reduce the volume of bone surrounding the cochlea before decalcification. When present, ossicles were removed and preserved in a 1% formalin solution for use in density measurements at a later date.

The periotic bones from the gross dissection were placed into solution to decalcify the hard tissue surrounding the cochlea to allow sectioning for microscopy. The ears were decalcified in 5% trichloroacetic acid, ethylenediaminetetraacetic acid (EDTA), or in acid with later transfer to EDTA. Bone wax was placed in the oval and round windows of specimens decalcified in acid to reduce the impact of the acid on the soft tissues of the cochlea. Acid decalcification of various durations were attempted to determine whether this method is acceptable to decrease time for decalcification and to determine the effects of acid techniques on inner ear structures, especially the basilar membrane.

After decalcification was complete, the ears were embedded in celloidin solution to harden and sectioned into 20- μ m sections. All sections were retained and every 10th section was stained with hematoxylin and eosin and mounted as cover-slipped slides (e.g., Fig. 7).

Basilar membranes that were present in the slide sections were measured for width and thickness (Fig. 8). The width was measured at a 40 \times objective magnification on a light microscope (Olympus Model BX40) with a graticule and ocular (10 \times) calibrated scale for width measurements. Oil immersion microscopy using a 100 \times oil immersion objective was used to measure basilar membrane thickness. Reconstructions of the basilar membranes were made using measurements of the basilar membranes from the slides and fitting them to an equiangular spiral with the same (α) value calculated for

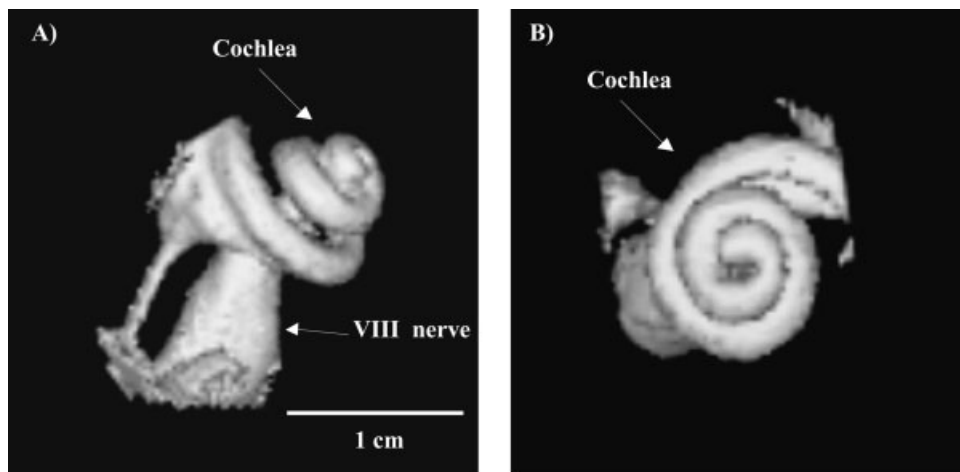


Fig. 3. A three-dimensional (3D) reconstruction of the cochlea from specimen EG 6. **A:** Lateral view showing the height of the right whale cochlea spiral and the VIIIth cranial nerve. **B:** View of the cochlear spiral illustrating the number of turns in the right whale cochlea, with 2.3 turns present in this specimen.

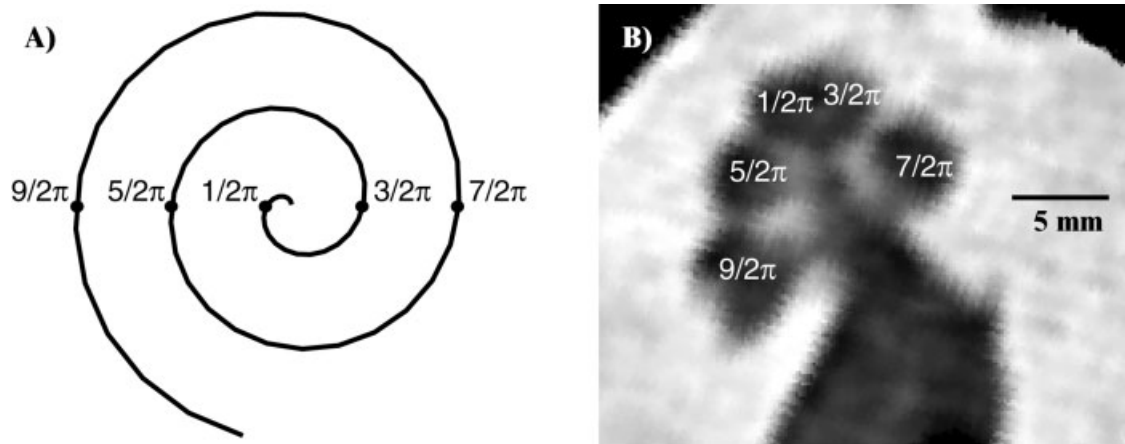


Fig. 4. Cross-section through a right whale cochlea for computerized tomography (CT) measurements. **A:** Schematic showing the orientation of the cross-section. **B:** An example of the resulting two-dimensional CT image from the cross-section.

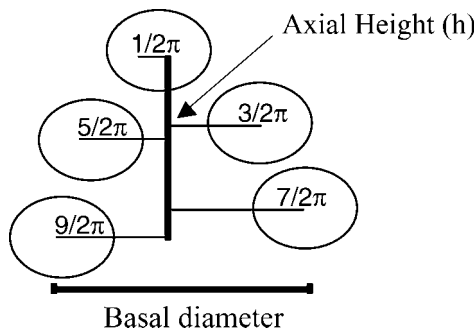


Fig. 5. Illustration of the measurements made from two-dimensional computerized tomography cross-sections from right whale specimens with 2.5 turns.

the right whale ears. Figure 9 shows the measurements of intact basilar membranes fit onto a curve.

Using the measured thickness and width of the basilar membrane at multiple positions along its length, the absolute and functional hearing range of the right whale can be estimated using the model described originally for odontocetes (Ketten and Wartzok, 1990) that is now conventionally used for human CT data (Ketten et al., 1998) and has been applied to mysticetes (Ketten, 1994). The functional hearing range is generally somewhat narrower than the total possible inner ear response range.

Ganglion cells were counted from each slide from all sectioned specimens, and total number of ganglion cells and total number of ganglion cell nuclei were counted at $40\times$ resolution using a grid. The number of ganglion cells counted from the mounted slide sections were multiplied by 10 (to account for the unmounted sections) (Schuknecht, 1993). The Konigsmark correction was used to avoid double counts from cells split between sections (Nadol, 1988: $N_{\text{corr}} = N_{\text{count}} [t / t + d]$ where N_{corr} = corrected cell count, N_{count} = actual cell count, t = thickness of the section and d = diameter of the cell counted). In this case, the thickness of the section = $20 \mu\text{m}$ and

the diameter of the cells is approximately $20 \mu\text{m}$ (range, $15 \mu\text{m}$ to $25 \mu\text{m}$), leading to a correction factor of 0.5.

All specimens show signs of decomposition and loss of ganglion cells. Therefore, combined counts pooling the highest ganglion cell counts for a given basilar membrane position from all specimens were used to estimate the total number of ganglion cells present in a right whale ear. The ganglion cell density/mm was calculated as a percentage of the basilar membrane length for the two specimens with the best preservation. The density counts from these two specimens were also pooled to get a better estimate of the density of ganglion cells per unit length of the basilar membrane.

RESULTS

CT Measurements

Initial surveys of cochlear dimensions from CT images showed that precise orientation of the cross-sections taken by the CT scanner is important for consistent measurement of all cochlear features of right whale cochlea (Table 2). The calculated cochlear length and the cochlear length measured directly from 3D CT reconstructions are shown in Table 3. There was good agreement between the predicted and observed cochlear length for most specimens. However, the values measured from the CT images are slightly longer. The added length is attributable to both minor shrinkage in sectioned material and to inclusion of the terminal hook in the measurements from the CT images.

Gross Dissection

There were several aspects of the temporal bone anatomy seen in all dissected specimens that are noteworthy. First, the juncture between the petiotic and tympanic bones is extremely stable, with 2- to 5-mm thickness of bone providing two points of connection. The largest contact point, directly lateral of the cochlea itself, was often 1–2 cm in length. The second connection, at the anterior end of the petiotic, was generally smaller and thinner. These two connections formed an arch between the petiotic and tympanic through which the “glove finger”

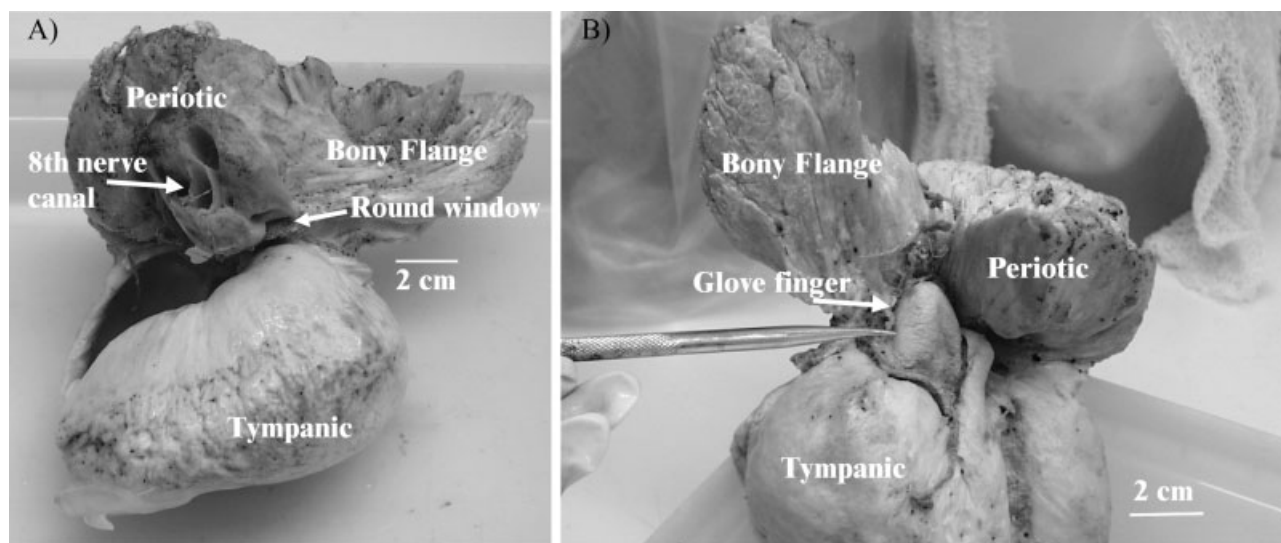


Fig. 6. Images from dissection of EG 11 temporal bones. **A:** The medial view of the right ear. The tympanic and periotic bones are labeled. The VIIIth cranial nerve canal, round window, and bony flange are also labeled. **B:** The lateral view of the same ear. The tympanic,

periotic, and flange are labeled to aid in orientation. The glove finger, which is the common term for the baleen whale tympanic membrane, is in its normal position between the two temporal bone elements.

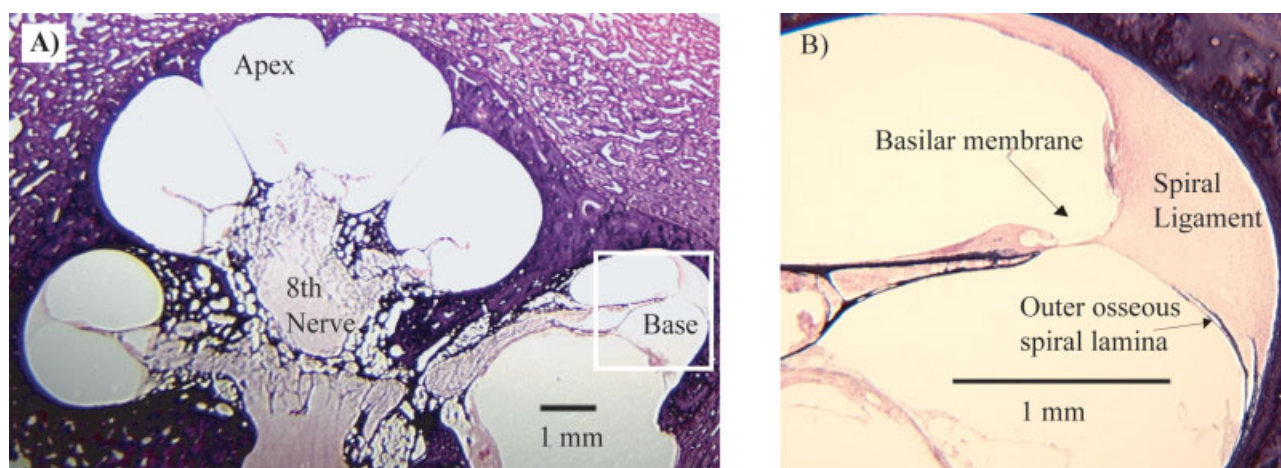


Fig. 7. Images from histology slide preparations from specimen EG 9. **A:** A mid-modiolar cross-section showing the layout of a right whale cochlea. The basal and apical turns are labeled. The VIIIth cranial nerve is also labeled. The basal turn is marked by a white square. **B:** The basal turn from under higher (15 \times) magnification. The basilar

membrane, spiral ligament, and outer osseous spiral lamina are labeled. Many inner ear structures are absent (e.g., Reissner's membrane separating the scala vestibuli and scala media) as a result of postmortem changes and histology preservation and decalcification.

(a derivative of the tympanic membrane) projected laterally (Fig. 6).

The entire ossicular chain was present in most specimens (Fig. 2). The malleus was supported by a bone strut that connected to the outer wall of the tympanic bone, close to the insertion of the glove finger. The corpus cavernosum covered the interior of the tympanic bone in three of four specimens. A spongy layer of sharp spicules of cancellous bone and fatty tissue covered the dorsal-lateral side of the periotic bone. This spongy layer was very difficult to remove from the specimens, and it covered a dome of very dense bone in the periotic

that projected laterally from the side of the cochlear duct itself. This very dense layer of bone was one of the major roadblocks to decalcification in these specimens. This dense bone and spongy pad correspond to a position immediately between the bony flanges that wedge the ears against the skull.

Histology Measurements

Acid decalcification produced multiple artifacts. Mid-modiolar cross-sections show the impact of the acid decalcification (Fig. 10). Comparing the preparations of EG 1

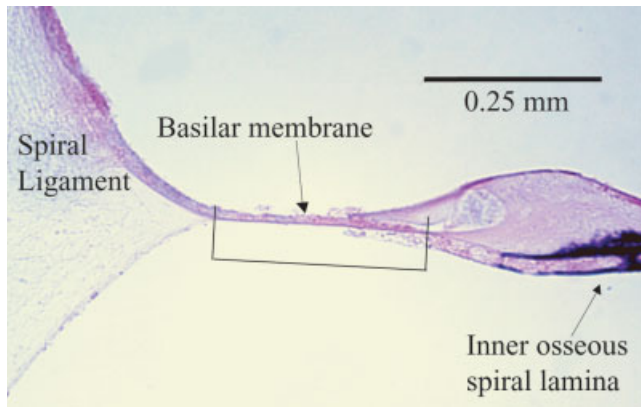


Fig. 8. Basilar membrane from EG 9 at 20× marking points for measurement of the width of the membrane. The thickness of the membrane was measured in the center of the membrane.

(no acid) (Fig. 10A) and EG 18 (only acid) (Fig. 10D) illustrates the effect of acid decalcification. There is clear decalcification of the bone surrounding the cochlea from EG 18, and all of the inner osseous spiral laminae have been dissolved, resulting in total disruption of any basilar membrane that may have remained when the specimen was collected.

Ganglion cells. The preservation of ganglion cells varied in the specimens sectioned for slides. The total corrected ganglion cell count for the two specimens with the best preservation are 37,930 for EG 4 and 31,390 for EG 9. This finding represents a minimum estimate of cells as there is clear evidence of neuronal loss from disease and/or decomposition in these specimens. A count of 45,250 is obtained by combining the highest ganglion cell count for a particular position on the basilar membrane from EG 4 and EG 9. Calculation of the ganglion cell density/mm results in an average value of 1,842 ganglion cells/mm (Table 4), which is likely to be a more

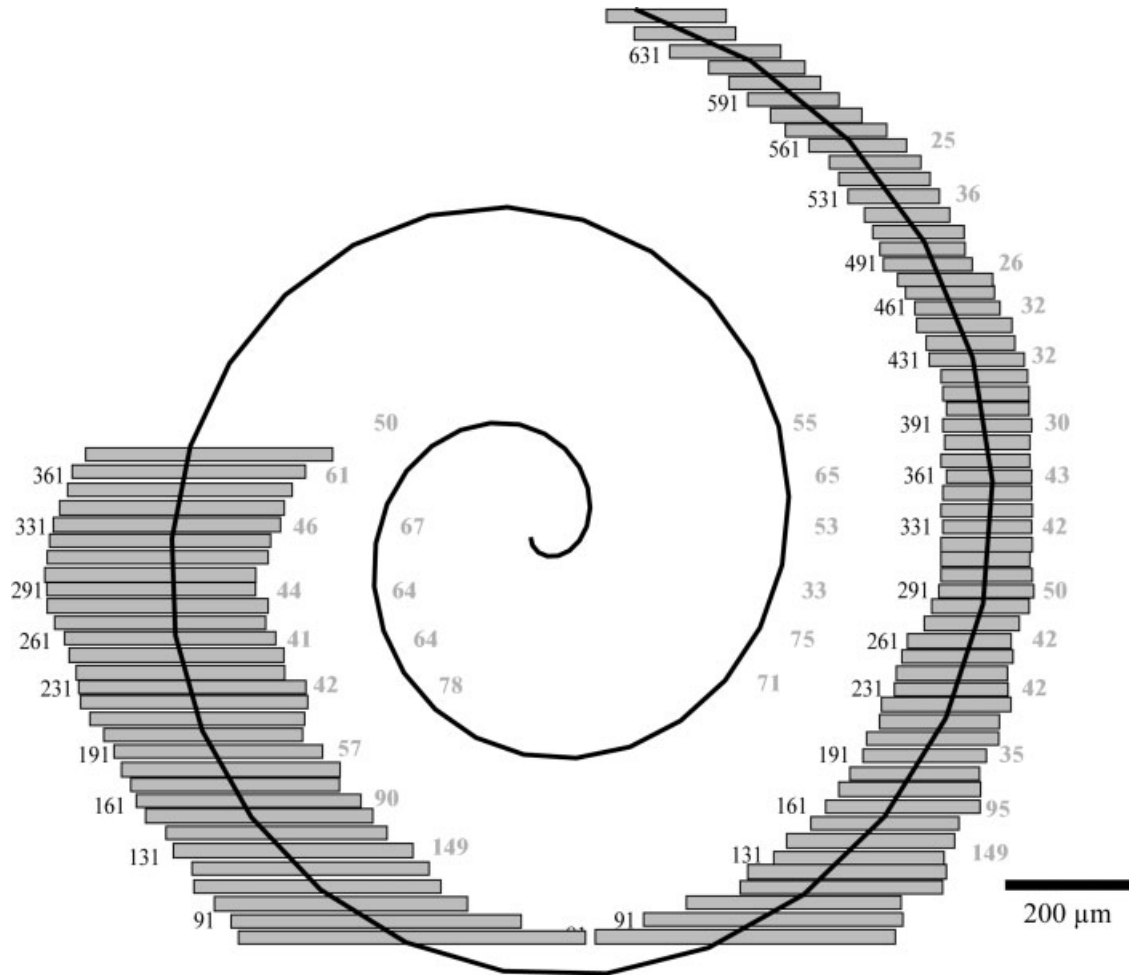


Fig. 9. Image of a reconstructed basilar membrane with ganglion cell counts from the slide measurements. The gray bars represent the length of the basilar membrane at particular points on the cochlea. The black numbers represent the slide number. The light gray numbers are the count of ganglion cells at each point on the corresponding slide.

TABLE 2. Radii measurements taken from the computed tomography scans for all specimens^a

	$1/2 \pi$	$3/2 \pi$	$5/2 \pi$	$7/2 \pi$	$9/2 \pi$	Axial height	Basal diameter	Number of turns	Axial pitch	Basal ratio
Minimum	0.94	1.55	2.49	3.21	4.27	5.44	7.69	2.25	2.18	0.62
Maximum	1.47	2.61	3.48	4.06	5.54	6.33	9.47	2.5	2.61	0.77
Average	1.16	2.05	2.93	3.63	4.96	5.80	8.59	2.46	2.36	0.68
SD	0.16	0.28	0.26	0.24	0.39	0.25	0.54	0.09	0.12	0.05

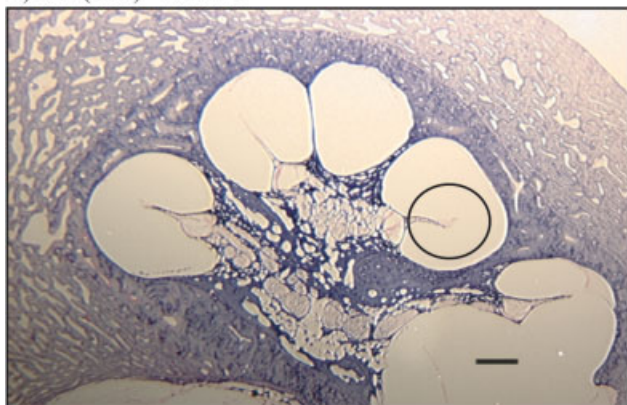
^aThe radii ($1/2 \pi$, $3/2 \pi$, $5/2 \pi$, $7/2 \pi$, and $9/2 \pi$ for 2.4–2.5 turns, 0 , π , 2π , 3π , and 4π for 2.25 turns), axial height and basal diameter are reported in millimeters. The number of turns is derived from counts made on three-dimensional reconstructions of the cochlea for each specimen. The axial pitch = axial height/number of turns, and the basal ratio = axial height/basal diameter defined by Ketten (1984).

TABLE 3. Measurements used for the calculation of length of the cochlear canal^a

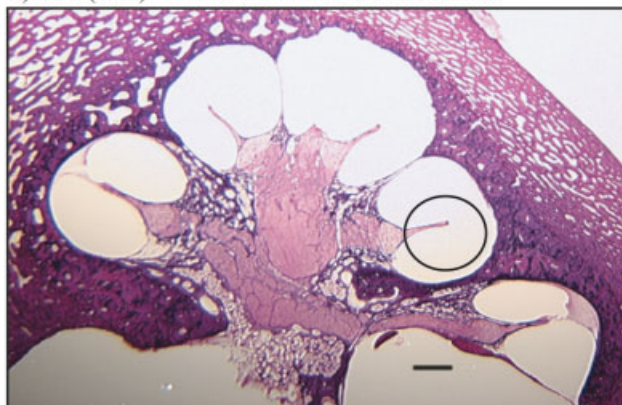
	Theta	Axial height	α = Spiral constant	z = Calculated cochlear length (mm)	Measured cochlear length (mm)
Minimum	14.14	5.44	0.41	50.54	52.11
Maximum	15.71	6.33	0.56	61.68	63.16
Average	15.43	5.80	0.46	55.67	56.97
SD	0.55	0.25	0.04	3.22	3.75

^aTheta is the number of degrees in the spiral reported in radians. Axial height is the height of the spiral in millimeters. The spiral constant (α) is calculated to give the relative size of the approximated spiral from formula (1). Calculated cochlear length (z) is calculated from formula (2).

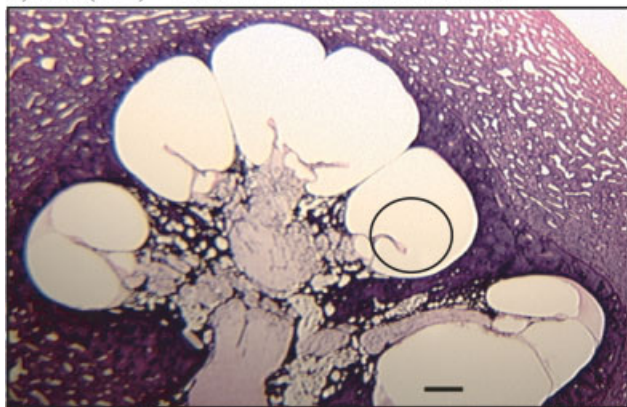
A) EG1(Calf) - No Acid



B) EG4 (Calf) - 2 Months in Trichloroacetic Acid



C) EG9 (Calf) - 1.5 Months in Trichloroacetic Acid



D) EG 18 (Adult) - 6 months in Trichloroacetic acid

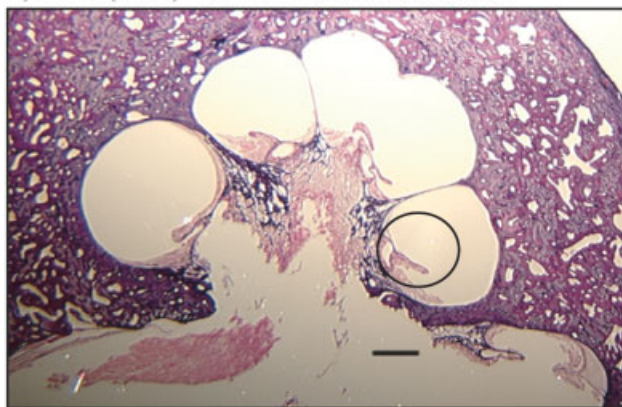


Fig. 10. Impact of acid decalcification on baleen whale ear bones. **A:** Ear from EG 1 (calf) decalcified in ethylenediaminetetraacetic acid (EDTA) only. **B:** Ear from EG 4 (calf), 2 months in trichloroacetic acid, 14 months in EDTA. **C:** Ear from EG 9 (calf), 1.5 months in trichloroacetic acid, 5 months EDTA. **D:** Ear from EG 18 (adult), 6 months in

acid decalcification with bone wax in the oval and round windows to reduce the time the tissues of the inner cochlea were exposed to acid. The start of the second turn is circled in each slide for comparison of the acid effects on the inner osseous spiral lamina. The scale bar in each image = 1 mm.

TABLE 4. Calculated ganglion cell density per millimeter of the basilar membrane

Percent membrane length	Highest ganglion cell density
5	625
10	900
15	1,525
20	3,075
25	1,225
40	2,850
45	1,600
50	2,875
70	1,575
75	2,900
90	1,675
98	1,275
Average density (ganglion cells/mm)	1,842

representative estimator of total population, when multiplied by length, than are the partial totals obtained in these tissues. Combined with the average cochlea length (55.7 mm, Table 3), the probable total ganglion cell number is approximately 102,500 ganglion cells, assuming equal neuronal distribution throughout the length of the basilar membrane. The lower actual counts in this study are clearly the result of cellular loss from specimen decomposition as well as possible in vivo pathologies.

Basilar membrane measurements and predicted frequency range of hearing. All specimens had measurable intact membranes in some region of the cochlea. The wider, thinner membranes near the apical turn of the cochlea were often poorly preserved, while the shorter, thicker portion of the membrane supported by the outer osseous spiral laminae was intact for all specimens. Table 5 shows the thickness/width ratios at different sections of the membrane length and the estimated frequency range of hearing for the right whale calculated from the data using the model described in Ketten (1994). These numbers represent the functional range of the average of the ears measured in this study. These values also indicate a total possible hearing range of the right whale of approximately 10 Hz–22 kHz.

DISCUSSION

The results of this study provide a description of North Atlantic right whale ear morphology and measurements of their cochlear and basilar membrane dimensions. The highly endangered status of the North Atlantic right whale has resulted in concerted efforts to perform complete necropsies on all dead right whales that can be recovered. This has resulted in the collection of baleen whale ears that are in good condition when from relatively fresh specimens. Better specimens could be collected from fresh kills in populations of baleen whales where whaling still occurs. This is not an option for any right whale population anywhere in the world.

This study indicates that collection of ear bones from right whales in any state of decomposition is worthwhile. This may have great application to collection of

TABLE 5. Thickness/width ratio of the basilar membrane measurements and predicted frequency response at different percentages of membrane length (apex = 0) combined from measurements from four individual specimens^a

% Membrane length (apex to base)	Thickness/width ratio	Predicted frequency (kHz)
2	0.0012	0.012
20	0.0019	0.093
50	0.0125	1.44
80	0.0357	13.42
83.5	0.0425	13.67
90	0.05	18.28

^aThe thickness/width ratio was only measured from nontangential sections.

specimens from other species for which research approaches are similarly limited. Ears collected from highly decomposed specimens often retained the ossicular chain position in situ. Specimens with moderate decomposition retained the tough glove finger and lining of the tympanic chamber. All specimens allowed for measurement of size, length, and number of turns in the cochlea of the right whale. Decalcification and histological processing of two Code 3 (moderate decomposition) specimens resulted in very useful basilar membrane measurements and ganglion cell counts. Specimens in any condition from other right whale populations would be of use to determine whether there are significant differences in ear anatomy among the three proposed species of right whales.

CT Measurements

The CT scanning of specimens proved effective for a variety of in situ measurements of right whale ears. Both 2D and 3D images were useful in describing the right whale cochlea. The 2D reconstructions were used to evaluate the condition of the middle ear and to detect any remnants of the VIIIth cranial nerve and in some cases the basilar membrane condition to assist with selection for further dissection and histological processing. Cochlear length could be determined both from measurement of radii from 2D cross-sections and from direct measurement of 3D reconstructions of the canal. The total number of turns was best determined from the 3D reconstructions.

The dimensions, position, and orientation of other ear structures are simultaneously available from CT scans of intact ears, including the vestibular system and ossicles (Fig. 2). Measures of these structures will allow for future estimates of middle ear transfer functions for this species. Scans of entire temporal complexes could be used for measurement of the size of the tympanic and the periotic bones. All of these observations can be made without disturbing the positions or destroying the specimen.

Gross Dissection and Histology

The gross dissections of ears provided data relating to middle ear structures in the bony ear complex of right

whales. The spongy cancellous bone covering the densest dome of bone of the periotic may provide insight into the mode of sound transduction in right whales (see also Nummela et al., 2007, this issue). If bone conduction of sound is important for hearing in right whales, then the flanges may function to direct the sound to the dense bone surrounding the cochlea, with the spongy pad reducing incoming bone conduction of sound from other directions. Alternatively, the spongy pad of bone against the very dense bone surrounding the cochlea could function to isolate the cochlea from vibrations of the skull. The bony strut found supporting the ossicles and the presence of a well-developed stapodial muscle indicate that the ossicular chain in right whales may be functional. Even with the strut and the muscle present, the ossicular chain can be moved. Further mechanical studies need to be conducted to determine the functional role of the ossicles in baleen whale hearing.

Decalcification times for right whale ears was longer than would be predicted simply from the mass of the ears, primarily because of the exceptional density of the periotic, the bone surrounding the cochlea. Decalcification of an isolated, pared down, periotic bone took from 6–20 months, depending on the size of the specimen and the time in acid. The 5% trichloroacetic acid was used in an attempt to accelerate the rate of decalcification. The acid did substantially increase the rate of decalcification. For example, EG 18's left ear decalcified in 6 months solely in acid, but EG 18's right ear took 20 months in EDTA. However, acid alone as a decalcificant created multiple and significant artifacts, including the loss of soft tissue within the cochlea (Fig. 10). In baleen whales, the width and thickness of the basilar membrane toward the apical turn is the most important feature for accurate measurements to estimate low frequency hearing sensitivity. Unfortunately, membranes in the apex are the most fragile and the first lost in acid decalcification. None of the specimens decalcified in acid retained any basilar membrane beyond the first turn of the cochlea. A chelating agent such as EDTA is far superior. EDTA minimizes artifacts from decalcification and better preserves fragile membranes (Schuknecht, 1993). There is evidence that even specimens decalcified in EDTA can be overdecalcified. The extremely dense section of bone that projected laterally from the cochlear canal was the last area to decalcify, and it is likely that the cochlear canal itself was sufficiently decalcified to allow cutting significantly earlier. Future attempts at decalcification should focus on removing as much of the high density periotic as possible before and during decalcification as more is exposed to accelerate the process. Specimens from calves and adults made it possible to observe aging effects, such as demineralization of the periotic bone in older whales. Figure 10a–c shows ears from calves (<6 months in age) while Figure 10d is an ear from an adult, at least 23 years of age. The latter has lower bone density surrounding the cochlea. This change is not merely a result of differences in decalcification of the preserved specimen, but rather a real density difference that was evident from CT scans before the ear was dissected and decalcified.

The basilar membrane dimensions of the right whale are consistent with previously described measurements of baleen whale basilar membranes (Wartzok and Ketten, 1999). The base of the basilar membrane is thicker

and narrower than the apical turn, which is extremely thin and wide. The apical turn of the right whale ear has membranes that may be thinner than can be accurately measured by traditional light microscopy and are perhaps best examined by transmission electron microscopy.

The distribution of ganglion cells in the best-preserved specimens indicates that there may be variable ganglion distribution and possibly hair cells in different regions in the cochlea of right whales. However, the postmortem decomposition of the specimens makes interpretation of the remaining ganglion cells difficult. Combining the counts of the best preserved sections of the basilar membranes from EG 4 and EG 9 still yielded a total ganglion cell count that was significantly lower than any reported ganglion cell count for any cetacean species due to large segments with total loss of cells. The direct counts are slightly greater than seen in human ears (30,000) but much less than half of what has been reported for other baleen whales (156,000) (Ketten, 2000). The density of cells in relatively well preserved areas was consistent with previous cetacean ganglion cell data (Ketten, 2000). The estimated ganglion cell densities/mm coupled with the average length of the right whale basilar membrane yielded a count comparable to those of other cetaceans. It is notable that the ganglion cell count of the right whale, presented here, and other baleen whales rival those of odontocetes and these counts are much higher than the average for any terrestrial mammal (Ketten, 2000).

The total hearing range for the right whale predicted from measurements presented here is 10 Hz–22 kHz with functional ranges probably being 15 Hz–18 kHz. These estimates were made using the model described in Ketten (1994). The model has been shown to accurately predict the frequency range of hearing in both odontocetes and bat species. Currently, there are no direct measures of baleen whale hearing; therefore, the results from this model cannot be compared with behavioral or physiological hearing curves for right whales. The robustness of this model makes it likely that the frequency range of hearing presented here is a close approximation to the hearing abilities of this species. The apical measurements of the basilar membrane indicate better low frequency hearing than in humans, while the capacity suggested by the basal end of the membrane is slightly higher in frequency but similar to human ears. As expected, this range corresponds well to the sounds produced by right whales (Parks and Tyack, 2005). Both this frequency range and the frequency range of right whale sounds overlap with the frequency range of many anthropogenic noise sources, suggesting that noise could potentially have a negative impact on hearing, localization, and communication by right whales.

This study represents a rare look at multiple ear specimens from a single baleen whale population. It provides a comprehensive description of multiple ear specimens collected from an endangered baleen whale species. It is difficult to collect baleen whale ear specimens as large whale strandings are relatively rare in comparison to those of small odontocetes. As expected, there was variation in the size, length, and number of turns of cochlea from different individuals, but consistent intraspecies spiral form and length. Further research is

needed to ground-truth these model predictions with field tests of the functional upper frequency of hearing of right whales and the relative sensitivity of right whales.

ACKNOWLEDGMENTS

The specimens used in this study were collected with the assistance of numerous research staff and volunteers. Sincere thanks to everyone involved in the specimen collection, including M. Moore, the Cape Cod Stranding Network, the Mid-Atlantic Stranding Network, and the New England Aquarium right whale research group. Members of the Ketten laboratory, particularly S. Cramer and J. Fenwick, at the Woods Hole Oceanographic Institution provided support and assistance with the project. P. Tyack supported S.E.P. during her graduate work and provided constructive suggestions and comments during all stages of this work. S.E.P. was supported in part by a NDSEG Fellowship and the Woods Hole Oceanographic Institution Education Office.

LITERATURE CITED

- Au WWL. 2000. Hearing in whales and dolphins: an overview. In: Au WWL, Popper AN, Fay RR, editors. Hearing by whales and dolphins. New York: Springer-Verlag. p 1–42.
- Clark CW, Clark JM. 1980. Sound playback experiments with southern right whales (*Eubalaena australis*). *Science* 207:663–665.
- Cummings WC, Thompson PO. 1971. Gray whales, *Eschrichtius robustus*, avoid the underwater sounds of killer whales, *Orcinus orca*. *Fish Bull* 69:525–530.
- Echteler SW, Fay RR, Popper AN. 1994. Structure of the mammalian cochlea. In: Popper AN, editor. Comparative hearing: mammals. New York: Springer-Verlag. p 134–171.
- Fay RR. 1992. Structure and function in sound discrimination among vertebrates. In: Popper AN, editor. The evolutionary biology of hearing. New York: Springer-Verlag. p 229–267.
- Frankel AS, Joseph R, Mobley J, Herman LM. 1995. Estimation of auditory response thresholds in humpback whales using biologically meaningful sounds. In: Kastelein RA, Thomas JA, Nachtigall PE, editors. Sensory systems of aquatic mammals. Woerden, The Netherlands: De Spil Publishers. p 55–70.
- Greenwood DG. 1961. Critical bandwidth and the frequency coordinates of the basilar membrane. *J Acoust Soc Am* 33:1344–1356.
- Greenwood DG. 1962. Approximate calculation of the dimensions of traveling-wave envelopes in four species. *J Acoust Soc Am* 34:1364–1384.
- Greenwood DG. 1990. A cochlear frequency-position function for several species—29 years later. *J Acoust Soc Am* 87:2592–2605.
- Hamilton PK, Martin SM. 1999. A catalog of identified right whales from the Western North Atlantic: 1935 to 1997. Boston: New England Aquarium, Central Wharf. 27 p + 382 plates.
- Kenney RD, Kraus SD. 1993. Right whale mortality - a correction and an update. *Mar Mammal Sci* 9:445–446.
- Ketten D. 1984. Correlations of morphology with frequency for Odontocete cochlea: systematics and topology. Baltimore: The Johns Hopkins University.
- Ketten DR. 1992. The marine mammal ear: specializations for aquatic audition and echolocation. In: Webster D, Fay RR, Popper AN, editors. The evolutionary biology of hearing. New York: Springer-Verlag. p 717–754.
- Ketten DR. 1994. Functional analyses of whale ears: adaptations for underwater hearing. *I.E.E.E. Proc Underwater Acoust* 1:264–270.
- Ketten DR. 2000. Cetacean ears. In: Fay RR, editor. Hearing by whales and dolphins. New York: Springer-Verlag. p 43–108.
- Ketten DR, Skinner MW, Wang G, Vannier MW, Gates GA, Neely JG. 1998. In vivo measures of cochlear length and insertion depth of nucleus cochlear implant electrode arrays. *Ann Otolol Rhinol Laryngol* 107:1–16.
- Ketten DR, Wartzok D. 1990. Three-dimensional reconstructions of the dolphin ear. In: Kastelein R, editor. Sensory abilities of cetaceans. New York: Plenum Press. p 81–105.
- Knowlton AR, Kraus SD. 2001. Mortality and serious injury of northern right whales (*Eubalaena glacialis*) in the western North Atlantic. *J Cetacean Res Manage (Special Issue)* 2:193–208.
- Kraus SD. 1990. Rates and potential causes of mortality in North Atlantic right whales (*Eubalaena glacialis*). *Mar Mammal Sci* 6:278–291.
- Laist DW, Knowlton AR, Mead JG, Collet AS, Podesta M. 2001. Collisions between ships and whales. *Mar Mammal Sci* 17:35–75.
- Manley GA. 1971. Some aspects of the evolution of hearing in vertebrates. *Nature* 230:506–509.
- Moore MJ, Knowlton AR, Kraus SD, McLellan WA, Bonde RK. 2004. Morphometry, gross morphology and available histopathology in North Atlantic right whale (*Eubalaena glacialis*) mortalities (1970 to 2002). *J Cetacean Res Manage* 6:199–214.
- Nadol JB. 1988. Quantification of human spiral ganglion cells by serial section reconstruction and segmental density estimates. *Am J Otolarygol* 9:47–51.
- Nowacek DP, Johnson MP, Tyack PL. 2003. North Atlantic right whales (*Eubalaena glacialis*) ignore ships but respond to alerting stimuli. *Proc Biol Sci* 271:227–231.
- Nummela S, Thewissen JGM, Bajpai S, Hussain ST, Kumar K. 2007. Sound transmission in archaic and modern whales: anatomical adaptations for underwater hearing. *Anat Rec (this issue)*.
- Parks SE. 2003. Response of North Atlantic right whales (*Eubalaena glacialis*) to playback of calls recorded from surface active groups in both the North and South Atlantic. *Mar Mammal Sci* 19:563–580.
- Parks SE, Tyack PL. 2005. Sound production by North Atlantic right whales (*Eubalaena glacialis*) in surface active groups. *J Acoust Soc Am* 117:3297–3306.
- Richardson WJ, Greene CR Jr, Malme CI, Thomson DH. 1995. Marine mammals and noise. San Diego: Academic Press.
- Sales GD, Pye D. 1974. Ultrasonic communication by animals. London: Chapman and Hall.
- Schuknecht HF. 1993. Pathology of the ear. 2 ed. Philadelphia: Lea and Febiger.
- Tyack P. 1983. Differential response of humpback whales, *Megaptera novaeangliae*, to playback of song or social sounds. *Behav Ecol Sociobiol* 13:49–55.
- Urick RJ. 1983. Principles of underwater sound. Los Altos, CA: Peninsula Publishing.
- Wartzok D, Ketten DR. 1999. Marine mammal sensory systems. In: Reynolds JE III, Rommel SA, editors. Biology of marine mammals. Washington: Smithsonian Institution Press. p 117–175.
- Watkins WA. 1981. Activities and underwater sounds of fin whales. *Sci Rep Whales Res Inst* 33:83–117.
- Watkins WA. 1986. Whale reactions to human activities in Cape Cod waters. *Mar Mammal Sci* 2:251–262.
- West CD. 1985. The relationship of the spiral turns of the cochlea and the length of the basilar membrane to the range of audible frequencies in ground dwelling mammals. *J Acoust Soc Am* 77:1091–1101.